analytical chemistry

Article

Cite This: *Anal. Chem.* 2019, 91, 8532–8539

pubs.acs.org/ac

Determination of the Equilibrium Constant and Rate Constant of Protein–Oligonucleotide Complex Dissociation under the Conditions of Ideal-Filter Capillary Electrophoresis

An T. H. Le, Svetlana M. Krylova, and Sergey N. Krylov*

Department of Chemistry and Centre for Research on Biomolecular Interactions, York University, Toronto, Ontario M3J 1P3, Canada

Supporting Information

ABSTRACT: Ideal-filter capillary electrophoresis (IFCE) allows selection of protein binders from oligonucleotide libraries in a single step of partitioning in which protein-bound and unbound oligonucleotides move in the opposite directions. In IFCE, the unbound oligonucleotide does not reach the detector, imposing a problem for finding the equilibrium constant (K_d) and rate constant (k_{off}) of protein–oligonucleotide complex dissociation. We report a double-passage approach that allows finding K_d and k_{off} under the IFCE conditions, i.e. near-physiological pH and ionic strength. First, a plug of the protein–oligonucleotide equilibrium mixture passes to the detector in a pressure-driven flow, allowing for both the complex and free oligonucleotide to be detected as a single first peak. Second, the pressure is turned off and the voltage is applied to reverse the migration of only the complex which is detected as the second peak. The experiment is repeated with a lower voltage consequently resulting in longer travel time of the complex to the detector, greater extent of complex dissociation, and the decreased area of the second peak. Finally, the peak areas are used to calculate the values of K_d and k_{off}. Here we explain theoretical and practical aspects of the double-passage approach, prove its validity quantitatively, and, demonstrate its application to determine K_d and k_{off} for an affinity complex between a protein and its DNA aptamer. The double-passage approach for finding K_d and k_{off} of protein–oligonucleotide complexes under the IFCE conditions is a perfect complement for IFCE-based selection of protein binders from oligonucleotide libraries.

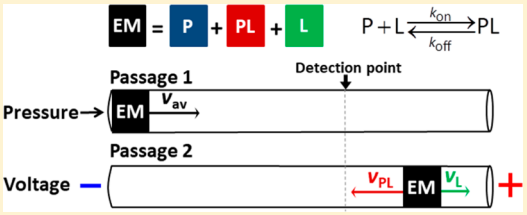

Selection of protein binders from oligonucleotide libraries, such as random-sequence oligonucleotide libraries and DNA-encoded libraries (DELs), can provide diverse pools of molecules for development of diagnostic probes and drugs.[1−7] Random- sequence oligonucleotide libraries are used to select aptamers, while DELs are used to select small-molecules, capable of binding target proteins. The low abundance of protein binders in oligonucleotide libraries makes it very hard to separate binders from nonbinders in a single step of partitioning.[8] As a result, multiple consecutive rounds of partitioning are typically used for in vitro selection of protein binders from oligonucleotide libraries.[9−16] In multiround selection of oligonucleotide aptamers, the number of rounds is theoretically unlimited, but a large number of rounds can lead to selection failure due to sequence biases of polymerases used to amplify oligonucleotides.[17−19] In selection of protein binders from DELs, the number of rounds is limited to three or four due to binder loss in partitioning and the inability to amplify the DNA-encoded small molecules by polymerases.[4,7] As a result of inefficiencies in typical multiround selections, 70 percent of attempts to select oligonucleotide aptamers fail,[3] and nonbinders dominate over binders in the enriched DELs.[20] An ultimate solution for these problems would be having a partitioning method that could enrich protein binders to the level of >90% of binders in the binder-enriched library in a single partitioning step.

We have recently introduced ideal-filter capillary electrophoresis (IFCE), in which protein-bound and unbound oligonucleotides move in the opposite directions inside the capillary.[21] The condition of IFCE is achieved when the magnitude of the mobility of electroosmotic flow (EOF) is smaller than that of protein–oligonucleotide complexes and larger than that of free oligonucleotides while the signs of the latter two mobilities are negative.[22] The efficiency of IFCE-based partitioning of binders from nonbinders reaches 10^9, which is 10^7 times greater than those of solid-phase partitioning methods and 10^4 times greater than that of homogeneous partitioning by capillary electrophoresis (CE) in which protein-bound and unbound oligonucleotides move in the same direction.[9−12,23−27] The classical CE-based partitioning is carried out at higher-than-physiological pH and lower-than-physiological ionic strength of the background electrolyte. Advantageously, the conditions of IFCE are achieved at near-physiological values of pH and ionic strength providing greater biological relevance of selected protein binders and suppressed nonspecific binding of the protein with the oligonucleotides and with the capillary surface. Partitioning by IFCE was shown to facilitate the one-step selection of DNA aptamers, and it

Received: April 12, 2019
Accepted: May 28, 2019
Published: May 28, 2019

DOI: 10.1021/acs.analchem.9b01801
Anal. Chem. 2019, 91, 8532–8539

promises to be applicable to selection of protein binders from DELs.

The movement of the unbound oligonucleotides away from the detection end of the capillary makes impossible their detection in IFCE. This creates a problem for measuring the equilibrium constant (K_d) and rate constant (k_{off}) of protein−oligonucleotide complex dissociation by IFCE. (It is worth mentioning that this problem does not exist in nonequilibrium capillary electrophoresis of equilibrium mixtures, in which protein-bound and unbound oligonucleotides move in the same direction.)[27] Here we describe a solution for this problem via double passage of the sample through the detection window: the first passage is driven by pressure, and the second passage is driven by an electric field.

The essence of the proposed double-passage approach is the following. The oligonucleotide is fluorescently labeled allowing for fluorescence detection of both free oligonucleotide and protein−oligonucleotide complex. A plug of the protein−oligonucleotide mixture at equilibrium is injected into the capillary from its close-to-the-detector end. The plug is moved slowly by pressure to and through the detection window and stopped after passing it. Since the protein-bound oligonucleotide is not separated from the unbound oligonucleotide in a slow pressure-driven flow, both contribute to the area of the first recorded peak. The voltage is then applied with a negative polarity being at the injection end of the capillary, and the protein-bound oligonucleotide moves back to the detector while the unbound oligonucleotide moves further away from the detector. Only the protein-bound oligonucleotide passes through the detector the second time and contributes to the area of the second recorded peak. The two peak areas are corrected for different velocities of pressure-driven migration and electric-field-driven migration. The relative quantum yield of the fluorescent label within the protein-bound oligonucleotide with respect to that of unbound oligonucleotide can be determined as a ratio of first-passage peak areas for pure oligonucleotide and near-pure complex that exists in the equilibrium mixture with protein concentration much greater than the value of K_d. Finally, the areas corrected for different velocities, different quantum yields, and also label photobleaching (if significant) are used to calculate accurate values of K_d and k_{off}.

In this work, general procedures for finding K_d and k_{off} are summarized, and the theory of the double-passage approach in the context of these general procedures is presented. Selection of suitable conditions for the pressure-driven stage is discussed. Good recoveries of peak areas and a fraction of unbound oligonucleotide were demonstrated using a model system of noninteracting green fluorescent protein (GFP) and a fluorescently labeled oligonucleotide mixed at different ratios. Finally, the double-passage approach was utilized to find K_d and k_{off} values for an affinity complex between MutS protein and its DNA aptamer. The double-passage approach provides a solution for accurate determination of K_d and k_{off} of protein−oligonucleotide complexes under the near physiological conditions of IFCE. This kind of measurements is impossible in regular kinetic CE modes, such as nonequilibrium capillary electrophoresis of equilibrium mixtures, which are carried out at higher-than-physiological pH and lower-than-physiological ionic strength. Being a separation-based method, the double-passage approach requires reasonably large difference between the mobilities of the protein-oligonucleotide complex and the unbound oligonucleotide. Advantageously, virtually any protein will introduce a sufficient "mobility shift" for any oligonucleotide from a DEL or a random-sequence DNA library.[28−30] Therefore, the double-passage approach is robust to variation in sizes of the protein and the oligonucleotide. Protein adsorption onto the inner capillary wall has detrimental consequences in CE-based measurements of K_d and k_{off}.[31,32] The double-passage approach is the least sensitive to effects of protein adsorption among the CE-based methods for two reasons. First, the higher ionic strength of the running buffer in IFCE is expected to suppress protein adsorption on the capillary wall. Second, the method does not rely on peak shapes making it immune to at least moderate reversible protein adsorption. The double-passage approach for finding K_d and k_{off} of protein−oligonucleotide complexes under IFCE conditions is a perfect complement for IFCE-based one-step partitioning of protein binders from oligonucleotide libraries.

RESULTS AND DISCUSSION

General Procedures for Finding K_d and k_{off}. Reversible binding of a protein (P) to an affinity ligand (L) with a formation of an affinity complex (PL) can be described by the following equation of reaction (see note S1 for a complete list of symbols used in this work):

$$\mathrm{P} + \mathrm{L} \underset{k_{off}}{\overset{k_{on}}{\rightleftarrows}} \mathrm{PL} \tag{1}$$

Complex stability is characterized by the equilibrium constant of complex dissociation (K_d) which is defined as

$$K_d = \frac{[\mathrm{P}]_{eq}[\mathrm{L}]_{eq}}{[\mathrm{PL}]_{eq}} \tag{2}$$

where $[\mathrm{P}]_{eq}$, $[\mathrm{L}]_{eq}$, and $[\mathrm{PL}]_{eq}$ are equilibrium concentrations of P, L, and PL, respectively.

In general, finding K_d requires the determination of a fraction R of unbound L in a mixture of L and P in the state of equilibrium with the initial concentrations $[\mathrm{L}]_0$ and $[\mathrm{P}]_0$:

$$R = \frac{[\mathrm{L}]_{eq}}{[\mathrm{L}]_0} \tag{3}$$

K_d can then be calculated using the following expression:

$$K_d = \frac{[\mathrm{P}]_0 - [\mathrm{L}]_0(1 - R)}{1/R - 1} \tag{4}$$

Finding K_d is associated with a systematic error that is minimal when the following relationships are satisfied:[33]

$$[\mathrm{L}]_0/K_d \le 1$$
$$[\mathrm{P}]_0/K_d \approx 1 \tag{5}$$

Because K_d is not known a priori, accurate determination of K_d may require measurement of R at different $[\mathrm{P}]_0$ and fitting the R vs $[\mathrm{P}]_0$ binding isotherm with their theoretical relationship while using K_d as a variable:

$$R = -\frac{K_d + [\mathrm{P}]_0 - [\mathrm{L}]_0}{2[\mathrm{L}]_0} + \sqrt{\left(\frac{K_d + [\mathrm{P}]_0 - [\mathrm{L}]_0}{2[\mathrm{L}]_0}\right)^2 + \frac{K_d}{[\mathrm{L}]_0}} \tag{6}$$

DOI: 10.1021/acs.analchem.9b01801
Anal. Chem. 2019, 91, 8532−8539

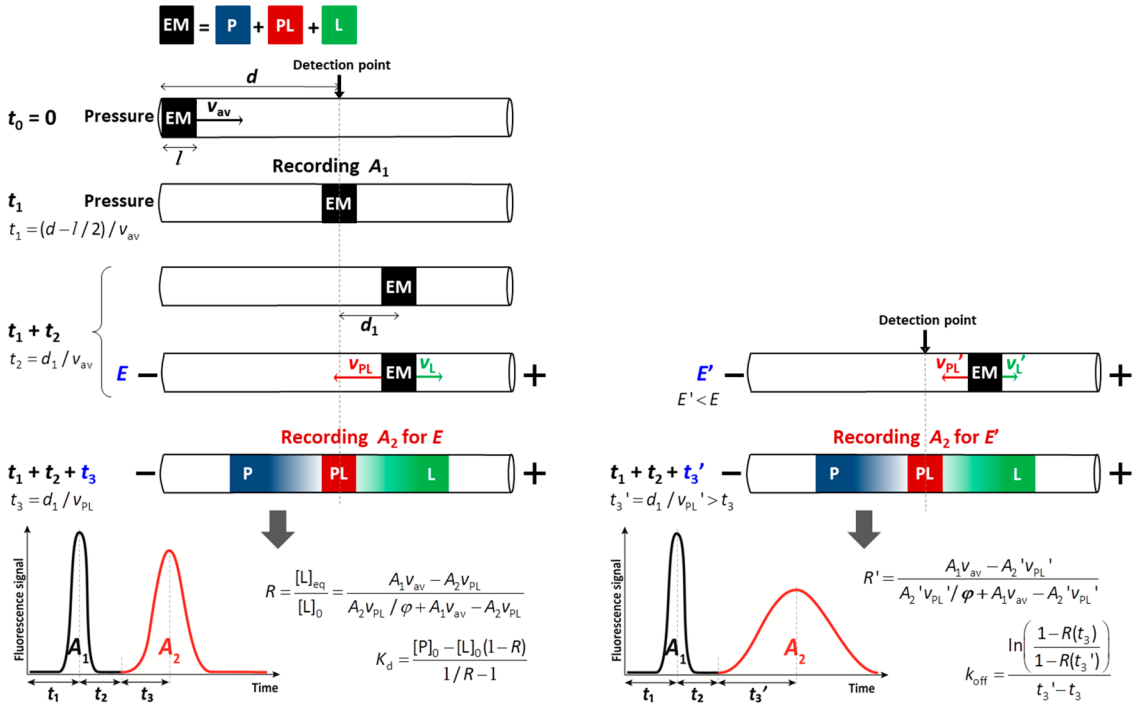

Figure 1. Schematic of the double-passage approach for finding K_d (left) and k_{off} (right) under the IFCE conditions. The pressure-driven step is identical for the left and right parts. See text for details.

Further, if the determined K_d does not satisfy the first inequality in eq 5, measurements should be repeated at a lower $[L]_0$.[33]

The determination of the rate constant of complex dissociation (k_{off}) requires inducing complex dissociation by physical separation of PL from L and P and measuring R as a function of time. The experimental dependence of $(1 - R(t))/(1 - R_{t=0})$ on time should then be fitted with the theoretical dependence:

$$\frac{1 - R(t)}{1 - R_{t=0}} = e^{-k_{off}t} \tag{7}$$

while using k_{off} as a fitting parameter. The complex-dissociation experiments should be conducted under conditions that minimize the rebinding reaction during the separation process. The rebinding can be neglected if a characteristic separation time of PL from the unbound L and P is much shorter than a characteristic rebinding time:

$$t_{sep} << t_{rebind} \tag{8}$$

When separation is carried out by CE, the characteristic separation time is defined via a plug length l, and velocity vectors $\mathbf{v}_{PL}$, $\mathbf{v}_L$, and $\mathbf{v}_P$ for PL, L, and P, respectively:

$$t_{sep} = \frac{l}{\max\{|\mathbf{v}_{PL} - \mathbf{v}_L|, |\mathbf{v}_{PL} - \mathbf{v}_P|\}} \tag{9}$$

For conditions of IFCE, $|\mathbf{v}_{PL} - \mathbf{v}_L| > |\mathbf{v}_{PL} - \mathbf{v}_P|$ and $|\mathbf{v}_{PL} - \mathbf{v}_L| = v_{PL} + v_L$, where v_{PL} and v_L are magnitudes (positive values) of the corresponding velocities. Thus, for the conditions of IFCE, eq 9 can be further specified:

$$t_{sep} = \frac{l}{v_{PL} + v_L} \tag{10}$$

The rate at which the rebinding reaction between P and L occurs during the separation process is directly proportional to the binding rate constant k_{on} and the concentration of unbound protein at equilibrium $[P]_{eq}$; the latter can be assumed to be approximately equal to $[P]_0$ for a typical condition of $[L]_0 \ll [P]_0$ used when finding k_{off}. The characteristic time of rebinding, t_{rebind}, thus, can be defined as

$$t_{rebind} = 1/(k_{on}[P]_{eq}) \approx 1/(k_{on}[P]_0) \tag{11}$$

Thus, minimizing rebinding of L formed from complex dissociation calls for minimizing $[P]_0$. On the other hand, a condition of $[P]_0 \gg [L]_0$ should still be satisfied, and the dynamic range of R should be sufficient for accurately measuring the kinetics of R increase upon complex dissociation. As a rule of thumb, $[P]_0 = K_d$ can be used for the determination of k_{off}. In such a case, $R_{t=0} = 1/2$, and the dynamic range of R is from 1/2 to 1. In general, it is practical to determine K_d first, which can require varying $[P]_0$, and, then, determine k_{off} at a single concentration of $[P]_0 = K_d$.

Theory of the Double-Passage Approach. The double-passage approach for finding K_d and k_{off} of protein–oligonucleotide complexes under the ICFE conditions is schematically illustrated in Figure 1. The equilibrium mixture (EM) of the protein (P) and the oligonucleotide that it binds (L) is prepared outside the capillary in the IFCE running buffer. A plug of EM of length l is injected into the capillary by pressure at a low flow velocity v_{av} to minimize plug elongation due to Taylor dispersion. The running buffer is then injected by pressure into the capillary at the same v_{av} to move the plug of EM through the detection window. Because the PL and L are not separated from each other in a slow pressure-driven flow, the area of the first recorded peak will represent a sum of equilibrium concentrations of PL and L:

$$A_1 = a(\varphi[PL]_{eq} + [L]_{eq})/v_{av} \tag{12}$$

DOI: 10.1021/acs.analchem.9b01801
Anal. Chem. 2019, 91, 8532–8539

where a is a coefficient of proportionality between the peak area and the concentration of the fluorescent oligonucleotide, and φ is a relative quantum yield of a fluorescent label within the protein−oligonucleotide complex with respect to that of the free oligonucleotide. The value of a is constant for the fixed geometry of the detection system, constant intensity of fluorescence−excitation light, and constant sensitivity of the photodetector. The value of φ is not expected to be much less than unity as the fluorophore is not involved in the protein−oligonucleotide binding reaction. The value of φ can be determined as a ratio between A_1 found for pure oligonucleotide ($[P]_0 = 0$) and A_1 for near-pure complex (the same $[L]_0$, but $[P]_0 \gg K_d$). The value of v_{av} can be calculated as

$$v_{av} = \frac{d - l/2}{t_1} \tag{13}$$

where d is the distance from the capillary inlet to the center of the detection window, and t_1 is time span from the beginning of EM plug propagation to the time when the plug's center reaches the center of the detection window.

The pressure-driven flow is stopped when the plug passes the detection window. The time span from the plug center's passing the center of detection window to the end of plug propagation is t_2, and the distance between the center of the stopped plug and the center of the detection window is

$$d_1 = v_{av} t_2 \tag{14}$$

The voltage is then applied with a negative polarity being at the injection end of the capillary. Under the conditions of IFCE, the protein-bound oligonucleotide moves back to the detector while the unbound oligonucleotide moves in the opposite direction, i.e. further away from the detector. Only PL passes through the detector the second time and contributes to the area of the second recorded peak. In the assumption of negligible complex dissociation during the second passage the area of the second peak is

$$A_2 = a\varphi[PL]_{eq}/v_{PL} \tag{15}$$

where v_{PL} is the electrophoretic velocity of PL which can be determined as

$$v_{PL} = \frac{d_1}{t_3} \tag{16}$$

Here t_3 is time from the beginning of electrophoresis to the moment when the center of the plug of PL reaches the center of the detection window.

If the two peak areas are measured and v_{av}, v_{PL}, and φ are determined as described above, then the value of R can be calculated as (see note S2 for derivation):

$$R = \frac{[L]_{eq}}{[L]_0} = \frac{A_1 v_{av} - A_2 v_{PL}}{A_2 v_{PL}/\varphi + A_1 v_{av} - A_2 v_{PL}} \tag{17}$$

and used to determine K_d with eq 4. If the found value of K_d does not satisfy the first inequality in eq 5, the experiments should be repeated at a lower value of $[L]_0$.

The value of k_{off} can be determined in a series of experiments with $[P]_0$ and $[L]_0$ satisfying both inequalities in eq 5 and for varying $t_3 = v_{PL} d_1$ via changing either v_{PL} or d_1. The value of v_{PL} can be changed by changing the magnitude of vector $\mathbf{E}$ of the electric field. The value of v_{PL} is a scalar product of this vector and a sum of electrophoretic mobility vectors of PL, $\boldsymbol{\mu}_{PL}$, and EOF, $\boldsymbol{\mu}_{EOF}$, respectively:

$$v_{PL} = \mathbf{E}\cdot(\boldsymbol{\mu}_{PL} + \boldsymbol{\mu}_{EOF}) \tag{18}$$

The value of d_1 can be changed by propagating the plug of EM further from the detector during the first passage. A two-point approach (with two different times of electrophoretic propagation: $t_3 < t_3'$) can be used for a simple assessment of k_{off} (see note S3 for derivation):

$$k_{off} = \frac{\ln\left(\frac{1 - R(t_3)}{1 - R(t_3')}\right)}{t_3' - t_3} \tag{19}$$

The found value of k_{off} should be used to assess if the rebinding could be neglected, i.e. if the inequality in eq 8 is satisfied. First, the value of k_{on} should be calculated with the found values of k_{off} and K_d:

$$k_{on} = k_{off}/K_d \tag{20}$$

This value of k_{on} should be used to calculate the characteristic rebinding time using eq 11. The value of v_L should be determined in a classical way by injecting a plug of pure L and propagating it to the detector by an electric field with a cathode at the injection end of the capillary and the magnitude of the electric field identical to that used in experiments utilized for finding K_d. If the migration time of the center of the plug of L to the center of the detector is t_4, then:

$$v_L = d/t_4 \tag{21}$$

If the found values of t_{sep} and t_{rebind} do not satisfy the inequality in eq 8, the experiments should be repeated with faster separation (smaller t_{sep}) which can be achieved by shortening the length l of the plug of EM and/or by increasing the differential velocity ($v_{PL} + v_L$) via increasing the electric field strength E, taking into account the proportionality of the differential velocity to E:

$$v_{PL} + v_L = E(\mu_{PL} + \mu_L) \tag{22}$$

where μ_{PL} and μ_L are magnitudes (positive values) of electrophoretic mobilities of PL and L, respectively.

Conditions for the First Passage. During the first, pressure-driven, propagation of the plug of EM to and through the detection window, equilibrium in the reversible binding reaction shown in eq 1 should not be perturbed significantly. In other words, the amounts of PL, L, and P should not change significantly during the pressure-driven propagation. The equilibrium will not be perturbed if the propagation time, which is defined in eq 13, is much shorter than the characteristic time of complex dissociation:

$$t_1 << 1/k_{off} \tag{23}$$

Because we do not know k_{off} a priori, it appears natural to use as small t_1 as can be achieved; however, small t_1 requires high v_{av} which inevitably leads to sample dilution due to Taylor dispersion and, thus, perturbed equilibrium. The dilution effect of Taylor dispersion becomes significant when:

$$v_{av} > \frac{l}{r^2/D} \tag{24}$$

where r is capillary radius and D is the diffusion coefficient of the largest-size analyte, which is PL in our case (r^2/D is the characteristic time of transverse diffusion of this analyte across

DOI: 10.1021/acs.analchem.9b01801
Anal. Chem. 2019, 91, 8532−8539

the capillary). Too high a value of v_{av} may even lead to transient incomplete separation (TIS) of L from PL, which produces a two-peak profile.[34,35] In addition to complicating data interpretation, TIS can potentially affect accuracy of quantitation due to radial nonuniformity of signal readout.[34] Thus, while no simple quantitative instruction can be given for an a priori choice of v_{av}, we suggest that TIS be avoided and satisfying eq 23 be tested when k_{off} is determined.

Recovery of Peak Areas. The double-passage approach measures velocity-corrected areas A_1v_{av} and A_2v_{PL} (see eq 17), where A_1 and A_2 are peak areas determined for "signal vs time" coordinates. The goal of this part of our study was to confirm that A_1v_{av} and A_2v_{PL} could be accurately determined using the approach for determination of v_{av} and v_{PL} described in Theory of the Double-Passage Approach. We used 1 μM GFP as an analyte mimicking PL in terms of electrophoretic mobility and the following default experimental parameters: d = 10.2 cm, r = 37.5 μm, l = 1.09 cm, pressure equal to 0.30 psi, total capillary length equal to 50 cm, and the electric field for carrying out the second passage being E = 200 V/cm. These default experimental parameters were used for all experiments in this work except for determination of k_{off} in which E' = 120 V/cm (see Figure 1, right) was used along with E = 200 V/cm.

The results of the peak-area recovery experiment are shown in Figure 2. The following five parameters were directly found

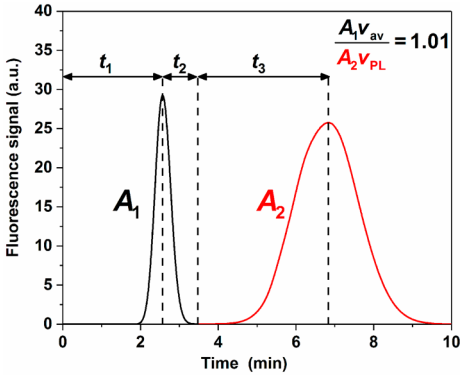

Figure 2. Determination of velocity-corrected peak areas via double-passage experiment. The sample mixtures contained 1 μM GFP in 50 mM Tris-HCl pH 7.0, 100 mM NaCl.

from this time dependence: t_1 = 171 s, t_2 = 56.0 s, t_3 = 201 s, A_1 = 8.69 × 10^7 a.u., and A_2 = 3.11 × 10^8 a.u. Then the value of v_{av} = 0.565 mm/s was found with eq 13, the value of d_1 = 3.16 cm was found with eq 14, and the value of v_{PL} = 0.0157 mm/s was found with eq 16. The ratio between the velocity-corrected areas was found to be $A_1v_{av}/(A_2v_{PL})$ = 1.01 for the results shown in Figure 2. The experiment was repeated 10 times, and the average value was found to be $A_1v_{av}/(A_2v_{PL})$ = 1.00 ± 0.01 (Figure 2, note S4) suggesting perfect recovery of the velocity-corrected peak areas. It is important to emphasize that this ratio may be greater than unity in case of significant photobleaching of the fluorophore during the first passage. GFP is photostable, and its photobleaching under our illumination conditions was negligible.

Recovery of *R*. To prove the recovery of R experimentally, we modeled equilibrium mixtures of a protein−oligonucleotide binding pair by mixing GFP and a fluorescently labeled DNA at known values of [DNA]/[GFP] ranging from 0.08 to 4. The quantum yield of GFP with respect to that of DNA was determined by identically injecting and pressure-propagating identical-length plugs of equimolar solutions of GFP and DNA, measuring peak areas A_{GFP} and A_{DNA}, and finding their ratio in 10 repetitions (Figure S2):

$$\varphi = A_{GFP}/A_{DNA} = 0.11 \pm 0.01 \quad (25)$$

A double-passage experiment with GFP−DNA mixtures was carried out using the default experimental parameters. Time dependencies of the fluorescence signal are shown in Figure 3a.

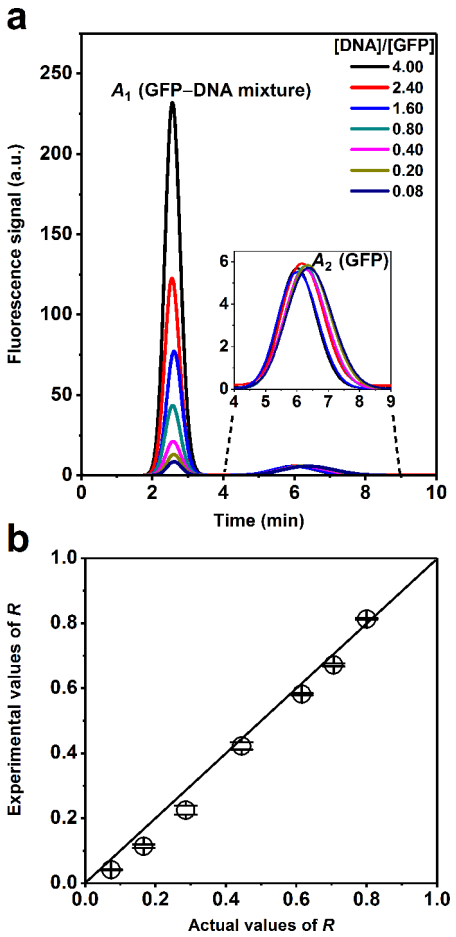

Figure 3. Recovery of R for double-passage experiments of GFP−DNA mixtures with [DNA]/[GFP] ranging from 0.08 to 4. Panel a shows time dependencies of fluorescence signal for different [DNA]/[GFP]. Panel b shows the comparison between the experimental and the actual values of R.

The values of t_1, t_2, t_3, A_1, and A_2 were found directly from these time dependencies (note S5). The values of secondary parameters v_{av}, d_1, and v_{PL} were calculated with eqs 13, 14, and 16, respectively (note S5). The found values of φ, A_1, A_2, v_{av}, and v_{PL} were used in eq 17 to calculate the values of R which were plotted against the actual values of R (Figure 3b). The recovery of R proved to be satisfactory for the entire range. The lower recovery at low concentrations of DNA were due to DNA adsorption on the walls of sample tubes.[36]

Experimental Determination of K_d and k_{off} of Protein−Aptamer Complex. In the final demonstration of analytical utility of the double-passage approach, we used an interacting pair of a protein (MutS) and its previously selected and characterized DNA aptamer.[33,37] An equilibrium mixture of MutS and the aptamer was prepared by mixing $[MutS]_0$ =

DOI: 10.1021/acs.analchem.9b01801
Anal. Chem. 2019, 91, 8532−8539

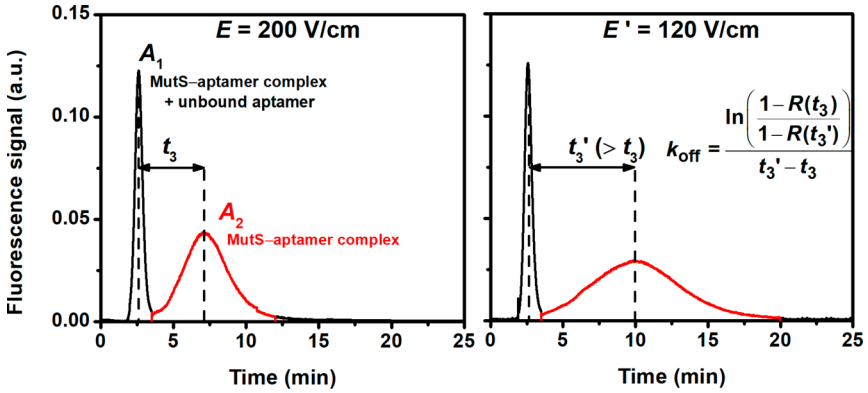

Figure 4. Double-passage experiment with a mixture of MutS protein and its aptamer under different electric field strengths: 200 and 120 V/cm. The sample mixture contained 0.50 nM MutS and 0.20 nM aptamer. The experiment was carrying out under using the default experimental parameters (see Materials and Methods).

0.50 nM with $[\text{aptamer}]_0$ = 0.20 nM and incubating the mixture for 1 h. The mixture was sampled for the double-passage experiment using the above-defined default experimental parameters. A typical time dependence of the fluorescence signal is shown in Figure 4, right. The experiment was repeated three times, and the values of t_1, t_2, t_3, A_1, and A_2 were found directly from these time dependences (note S6). The values of v_{av}, d_1, and v_{PL} were then calculated with eqs 13, 14, and 16, respectively (note S6). The found values of A_1, A_2, v_{av}, and v_{PL} were used in eq 17 to calculate R = 0.53 ± 0.01 under an assumption of φ = 1. The value of K_d = 0.47 ± 0.03 nM was then calculated with eq 4. The value of φ = 0.80 ± 0.01 was further calculated as a ratio between A_1 determined for near-pure complex and A_1 determined for pure aptamer (Figure S4). A more accurate value of R = 0.48 ± 0.01 was calculated with eq 17 using φ = 0.80. A φ-corrected value of K_d = 0.36 ± 0.02 nM was calculated by using R = 0.48 in eq 4.

The value of k_{off} was determined by using varying t_3 via changing the electric field strength. Along with the default value of E = 200 V/cm, we used a lower value of E' = 120 V/cm (Figure 4). Three experiments were carried out to find the values of t_3 = 225 ± 13 s for E = 200 V/cm and t_3' = 375 ± 17 s for E' = 120 V/cm. The value of $k_{off} = (1.1 \pm 0.5) \times 10^{-3}$ s^{-1} was calculated with eq 19.

We then carried out a quick test for our experiment's satisfying the inequality of eq 8. The value of v_L = 0.059 mm/s was determined by electrophoretically running a plug of pure L with a cathode at the inlet (Figure S6) and using eq 21. The value of t_{sep} = 54 s was calculated with eq 10. The value of $k_{on} = (3.0 \pm 1.2) \times 10^6$ M^{-1} s^{-1} was calculated with eq 20 by using the determined values of k_{off} and K_d. Finally, the value of t_{rebind} = 670 s was estimated with eq 11. Comparing t_{sep} and t_{rebind} suggests that the inequality of eq 8 was satisfied under our experimental conditions (54 ≪ 670) and, thus, the rebinding did not affect our determination of k_{off}.

Knowing k_{off} allowed us to make the final adjustment of K_d by taking into account the dissociation of PL during its electrophoretic migration to and through the detection window. Peak area $A_{2,t=0}$ corrected for this dissociation is

$$A_{2,t=0} = A_{2,t_3} e^{k_{off} t_3} \quad (26)$$

Using the corrected value of A_2 found from eq 26 in eq 17 for finding R and subsequently using the corrected R in eq 4, we found K_d = 0.20 ± 0.02 nM corrected for complex dissociation during the electrophoretic migration of PL to and through the detection window. The values of K_d = 0.20 nM and $k_{off} = 1.1 \times 10^{-3}$ s^{-1} determined by us under the IFCE conditions (ionic strength of 150 mM and pH 7.0) are very close to those determined for the same binding pair but at a much lower ionic strength of 13 mM and higher pH of 8.5: K_d = 0.1 nM and $k_{off} = 0.4 \times 10^{-3}$ s^{-1}.[33,37] This similarity suggests relative insensitivity of MutS–aptamer binding to ionic strength and pH.

To conclude, we developed the double-passage approach for determination of K_d and k_{off} of protein–oligonucleotide complex under the IFCE conditions (near-physiological ionic strength and pH). This approach is needed for assessing stability of protein–oligonucleotide complexes selected by IFCE. It will also be useful for assessing stability under the near-physiological conditions of protein–oligonucleotide complexes selected by nonequilibrium capillary electrophoresis of equilibrium mixtures under nonphysiological conditions.

MATERIALS AND METHODS

Materials. All chemicals and buffer components were purchased from Sigma-Aldrich (Oakville, ON, Canada) unless otherwise stated. Fused-silica capillaries with inner and outer diameters of 75 and 360 μm, respectively, were purchased from Molex Polymicro (Phoenix, AZ). Recombinant *A. victoria* GFP protein (MW ≈ 27 kDa, p*I* 5.7) was obtained from Abcam (Cambridge, UK). Recombinant *T. aquaticus* MutS protein (MW ≈ 90 kDa, p*I* 6.0) was expressed and purified as described previously.[38] All DNA molecules were custom synthesized by Integrated DNA Technologies (Coralville, IA). To study the recovery of R, a synthetic FAM-labeled DNA library (N40) with a 40-nt random region was used: 5′-FAM-CT ACG GTA AAT CGG CAG TCA-N40-AT CTG AAG CAT AGT CCA GGC. To determine K_d and k_{off} of a protein–aptamer pair, the DNA aptamer with affinity toward MutS protein was previously selected in our laboratory (clone 2-06),[37] and its Alexa Fluor 488-labeled version was used here: 5′-Alexa Fluor 488-CTT CTG CCC GCC TCC TTC CTG GTA AAG TCA TTA ATA GGT GTG GGG TGC CGG GCA TTT CGG AGA CGA GAT AGG CGG ACA CT-3′. A NanoDrop-1000 spectrometer (Thermo Scientific, Wilmington, DE) was used to determine concentrations of protein and DNA stock solutions by measuring light absorbance at 280 and 260 nm, respectively, and dividing the absorbance by the corresponding molar extinction coefficients. A solution of 5% bovine serum albumin was used to coat all the sample vials to

DOI: 10.1021/acs.analchem.9b01801
Anal. Chem. 2019, 91, 8532–8539

minimize absorption of DNA and protein onto the reservoir walls.[36] The CE running buffer was 50 mM Tris-HCl pH 7.0 supplemented with 100 mM NaCl. The sample buffer was always identical to the running buffer to prevent adverse effects of buffer mismatch. Accordingly, all dilutions of sample components used in CE experiments were done by adding the running buffer.

Experimental Procedures. Our default experimental parameters were: d = 10.2 cm, r = 37.5 μm, l = 1.09 cm, pressure for carrying out the first passage = 0.30 psi, total capillary length = 50 cm, and the electric field for carrying out the second passage E = 200 V/cm. These default experimental parameters were used for all experiments in this work except for measurements of k_{off} in which we also used a lower electric field strength of E' = 120 V/cm. Under our experimental conditions, magnitudes of electrophoretic mobilities of EOF, protein−oligonucleotide complex, and oligonucleotide were μ_{EOF} = 20, μ_{PL} = 13, and μ_L = 23 mm^2/(kV s).

All experiments were performed with a P/ACE MDQ apparatus (SCIEX, Concord, ON, Canada) capable of applying both pressure and electric field and equipped with a laser-induced fluorescence detection system. Fluorescence was excited with a blue line (488 nm) of a solid-state laser and detected at 520 nm using a spectrally optimized emission filter system.[39] An uncoated fused-silica capillary, with a total length of 50 cm and a 10.2 cm distance from one of the ends to the detection window was used. The temperature of the capillary coolant was set to 15 °C. Prior to every run, the capillary was rinsed successively with 0.1 M HCl, 0.1 M NaOH, deionized H_2O, and a running buffer for 3 min each under a pressure of 20 psi.

Mixtures of various concentration combinations were prepared, as described in Results and Discussion. Prior to the mixing, the DNA stock solution was incubated at 90 °C for 2 min and gradually cooled to 20 °C at a rate of 0.5 °C/s. For double-passage experiments with GFP−DNA mixtures, the concentration of GFP was 250 nM while the concentration of DNA ranged from 20 to 1000 nM (20, 50, 100, 200, 400, 600, and 1000). For experiments with MutS and its aptamers, the mixture was incubated at room temperature for 1 h. The prepared samples were injected into the capillary by a 0.3 psi ×17 s pressure pulse to yield a 1.09 cm-long sample plug inside the capillary. The injected sample plug was moved by pressure at 0.3 psi for 3.5 min. The pressure was then stopped, and either 10 or 6 kV was applied to the capillary ends (cathode at the injection end), resulting in electric field strengths of 200 or 120 V/cm, respectively. Peak areas and migration times were obtained by analyzing electropherograms with 32 Karat Software.

■ ASSOCIATED CONTENT

Supporting Information

The Supporting Information is available free of charge on the ACS Publications website at DOI: 10.1021/acs.analchem.9b01801.

Note S1: List of symbols; note S2: calculating R from the velocity-corrected peak areas via double-passage approach; note S3: calculating k_{off} from E during the second passage; note S4: recovery of peak areas; note S5: recovery of R; note S6: experimental determination of K_d and k_{off} of protein−aptamer complex; note S7: determination of v_L; Figures S1−S6; Tables S1−S3 (PDF)

Excel file with raw data and calculations (XLSX)

■ AUTHOR INFORMATION

Corresponding Author

*E-mail: skrylov@yorku.ca.

ORCID

An T. H. Le: 0000-0002-3659-9938

Svetlana M. Krylova: 0000-0002-3291-6721

Sergey N. Krylov: 0000-0003-3270-2130

Notes

The authors declare no competing financial interest.

■ ACKNOWLEDGMENTS

This work was supported by the Natural Sciences and Engineering Research Council of Canada (grant STPG-P 521331-2018).

■ REFERENCES

(1) Keefe, A. D.; Pai, S.; Ellington, A. *Nat. Rev. Drug Discovery* **2010**, *9*, 537−550.

(2) Dunn, M. R.; Jimenez, R. M.; Chaput, J. C. *Nat. Rev. Chem.* **2017**, *1*, No. 0076.

(3) Gold, L.; Ayers, D.; Bertino, J.; Bock, C.; Bock, A.; Brody, E. N.; Carter, J.; Dalby, A. B.; Eaton, B. E.; Fitzwater, T.; Flather, D.; Forbes, A.; Foreman, T.; Fowler, C.; Gawande, B.; Goss, M.; Gunn, M.; Gupta, S.; Halladay, D.; Heil, J.; Heilig, J.; Hicke, B.; Husar, G.; Janjic, J.; Jarvis, T.; Jennings, S.; Katilius, E.; Keeney, T. R.; Kim, N.; Koch, T. H.; Kraemer, S.; Kroiss, L.; Le, N.; Levine, D.; Lindsey, W.; Lollo, B.; Mayfield, W.; Mehan, M.; Mehler, R.; Nelson, S. K.; Nelson, M.; Nieuwlandt, D.; Nikrad, M.; Ochsner, U.; Ostroff, R. M.; Otis, M.; Parker, T.; Pietrasiewicz, S.; Resnicow, D. I.; Rohloff, J.; Sanders, G.; Sattin, S.; Schneider, D.; Singer, B.; Stanton, M.; Sterkel, A.; Stewart, A.; Stratford, S.; Vaught, J. D.; Vrkljan, M.; Walker, J. J.; Watrobka, M.; Waugh, S.; Weiss, A.; Wilcox, S. K.; Wolfson, A.; Wolk, S. K.; Zhang, C.; Zichi, D. *PLoS One* **2010**, *5*, No. e15004.

(4) Clark, M. A.; Acharya, R. A.; Arico-Muendel, C. C.; Belyanskaya, S. L.; Benjamin, D. R.; Carlson, N. R.; Centrella, P. A.; Chiu, C. H.; Creaser, S. P.; Cuozzo, J. W.; Davie, C. P.; Ding, Y.; Franklin, G. J.; Franzen, K. D.; Gefter, M. L.; Hale, S. P.; Hansen, N. J. V.; Israel, D. I.; Jiang, J. W.; Kavarana, M. J.; Kelley, M. S.; Kollmann, C. S.; Li, F.; Lind, K.; Mataruse, S.; Medeiros, P. F.; Messer, J. A.; Myers, P.; O'Keefe, H.; Oliff, M. C.; Rise, C. E.; Satz, A. L.; Skinner, S. R.; Svendsen, J. L.; Tang, L. J.; van Vloten, K.; Wagner, R. W.; Yao, G.; Zhao, B. G.; Morgan, B. A. *Nat. Chem. Biol.* **2009**, *5*, 647−654.

(5) Kleiner, R. E.; Dumelin, C. E.; Liu, D. R. *Chem. Soc. Rev.* **2011**, *40*, 5707−5717.

(6) Franzini, R. M.; Neri, D.; Scheuermann, J. *Acc. Chem. Res.* **2014**, *47*, 1247−1255.

(7) Goodnow, R. A.; Dumelin, C. E.; Keefe, A. D. *Nat. Rev. Drug Discovery* **2017**, *16*, 131−147.

(8) Berezovski, M.; Musheev, M.; Drabovich, A.; Krylov, S. N. *J. Am. Chem. Soc.* **2006**, *128*, 1410−1411.

(9) Ellington, A. D.; Szostak, J. W. *Nature* **1990**, *346*, 818−822.

(10) Tuerk, C.; Gold, L. *Science* **1990**, *249*, 505−510.

(11) Chen, H.; Gold, L. *Biochemistry* **1994**, *33*, 8746−8756.

(12) Nieuwlandt, D.; Wecker, M.; Gold, L. *Biochemistry* **1995**, *34*, 5651−5659.

(13) Quang, N. N.; Miodek, A.; Cibiel, A.; Ducongé, F. *Methods Mol. Biol.* **2017**, *1575*, 253−272.

(14) Navani, N. K.; Mok, W. K.; Yingfu, L. *Methods Mol. Biol.* **2009**, *504*, 399−415.

(15) Blind, M.; Blank, M. *Mol. Ther.–Nucleic Acids* **2015**, *4*, e223.

(16) Darmostuk, M.; Rimpelova, S.; Gbelcova, H.; Ruml, T. *Biotechnol. Adv.* **2015**, *33*, 1141−1161.

DOI: 10.1021/acs.analchem.9b01801
Anal. Chem. 2019, 91, 8532−8539

(17) Mutter, G. L.; Boynton, K. A. *Nucleic Acids Res.* **1995**, *23*, 1411−1418.
(18) Warnecke, P. M.; Stirzaker, C.; Melki, J. R.; Millar, D. S.; Paul, C. L.; Clark, S. J. *Nucleic Acids Res.* **1997**, *25*, 4422−4426.
(19) Takahashi, M.; Wu, X. W.; Ho, M.; Chomchan, P.; Rossi, J. J.; Burnett, J. C.; Zhou, J. H. *Sci. Rep.* **2016**, *6*, 33697.
(20) Arico-Muendel, C. C. GlaxoSmithKline, Cambridge, MA. Personal communication, February 6, 2019.
(21) Le, A. T. H.; Krylova, S. M.; Kanoatov, M.; Desai, S.; Krylov, S. N. *Angew. Chem., Int. Ed.* **2019**, *58*, 2739−2743.
(22) Le, A. T. H.; Krylova, S. M.; Krylov, S. N. Ideal-filter capillary electrophoresis: a highly efficient partitioning method for selection of protein binders from oligonucleotide libraries. *Electrophoresis*, published before the print https://doi.org/10.1002/elps.201900028.**2019** DOI: 10.1002/elps.201900028
(23) Irvine, D.; Tuerk, C.; Gold, L. *J. Mol. Biol.* **1991**, *222*, 739−761.
(24) Wang, J.; Rudzinski, J. F.; Gong, Q.; Soh, H. T.; Atzberger, P. J. *PLoS One* **2012**, *7*, No. e43940.
(25) Papoulas, O. *Curr. Protoc. Mol. Biol.* **2001**, 12.8.1−12.8.9.
(26) Ciesiolka, J.; Illangasekare, M.; Majerfeld, I.; Nickles, T.; Welch, M.; Yarus, M.; Zinnen, S. *Methods Enzymol.* **1996**, *267*, 315−335.
(27) Berezovski, M.; Drabovich, A.; Krylova, S. M.; Musheev, M.; Okhonin, V.; Petrov, A.; Krylov, S. N. *J. Am. Chem. Soc.* **2005**, *127*, 3165−3171.
(28) Bao, J.; Krylova, S. M.; Cherney, L. T.; Hale, R. L.; Belyanskaya, S. L.; Chiu, C. H.; Arico-Muendel, C. C.; Krylov, S. N. *Anal. Chem.* **2015**, *87*, 2474−2479.
(29) Bao, J.; Krylova, S. M.; Cherney, L. T.; Hale, R. L.; Belyanskaya, S. L.; Chiu, C. H.; Shaginian, A.; Arico-Muendel, C. C.; Krylov, S. N. *Anal. Chem.* **2016**, *88*, 5498−5506.
(30) Beloborodov, S. S.; Krylova, S. M.; Krylov, S. N. Spherical-Shape Assumption for Protein−Aptamer Complexes Facilitates Prediction of their Electrophoretic Mobility. *ChemRxiv* 2019, Preprint https://doi.org/10.26434/chemrxiv.8051921.v1.
(31) de Jong, S.; Krylov, S. N. *Anal. Chem.* **2012**, *84*, 453−458.
(32) de Jong, S.; Epelbaum, N.; Liyanage, R.; Krylov, S. N. *Electrophoresis* **2012**, *33*, 2584−2590.
(33) Kanoatov, M.; Galievsky, V. A.; Krylova, S. M.; Cherney, L. T.; Jankowski, H. K.; Krylov, S. N. *Anal. Chem.* **2015**, *87*, 3099−3106.
(34) Sisavath, N.; Rukundo, J. L.; Le Blanc, Y.; Galievsky, V.; Bao, J.; Kochmann, S.; Stasheuski, A.; Krylov, S. N. *Angew. Chem., Int. Ed.* **2019**, *58*, 6635−6639.
(35) Chamieh, J.; Leclercq, L.; Martin, M.; Slaoui, S.; Jensen, H.; Østergaard, J.; Cottet, H. *Anal. Chem.* **2017**, *89*, 13487−13493.
(36) Kanoatov, M.; Krylov, S. N. *Anal. Chem.* **2011**, *83*, 8041−8045.
(37) Drabovich, A. P.; Berezovski, M.; Okhonin, V.; Krylov, S. N. *Anal. Chem.* **2006**, *78*, 3171−3178.
(38) Beloborodov, S. S.; Bao, J.; Krylova, S. M.; Shala-Lawrence, A.; Johnson, P. E.; Krylov, S. N. *J. Chromatogr. B: Anal. Technol. Biomed. Life Sci.* **2018**, *1073*, 201−206.
(39) Galievsky, V. A.; Stasheuski, A. S.; Krylov, S. N. *Anal. Chem.* **2017**, *89*, 11122−11128.

DOI: 10.1021/acs.analchem.9b01801
Anal. Chem. 2019, 91, 8532−8539

Determination of the Equilibrium Constant and Rate Constant of Protein–Oligonucleotide Complex Dissociation under the Conditions of Ideal-Filter Capillary Electrophoresis

An T. H. Le, Svetlana M. Krylova, , Sergey N. Krylov*

Department of Chemistry and Centre for Research on Biomolecular Interactions, York University, Toronto, Ontario M3J 1P3, Canada

Supporting Information

For more information see also the Excel file in the Supporting Information.

Note S1: List of symbols

a	coefficient of proportionality between the peak area and the concentration of the fluorescent oligonucleotide
A_1	area of the first pressure-driven peak
A_2	area of the second electrophoretic peak
d	the distance from the capillary inlet to the center of the detection window
d_1	distance between the center of the stopped plug and the center of the detection window
D	diffusion coefficient of the largest-size analyte
$\mathbf{E}$	vector of the electric field
E	magnitude of $\mathbf{E}$
EM	equilibrium mixture
EOF	electroosmotic flow
k_{off}	rate constant of complex dissociation
k_{on}	rate constant of complex formation
K_d	equilibrium dissociation constant
l	length of sample plug
$[L]_0$	initial concentration of ligand
$[L]_{eq}$	equilibrium concentration of ligand
$\boldsymbol{\mu}_{EOF}$	electrophoretic mobility vector of electroosmotic flow
$\boldsymbol{\mu}_L$	electrophoretic mobility vector of ligand
μ_L	electrophoretic mobility of ligand
$\boldsymbol{\mu}_{PL}$	electrophoretic mobility vector of complex
μ_{PL}	electrophoretic mobility of complex
$[P]_0$	initial concentration of protein
$[P]_{eq}$	equilibrium concentration of protein
$[PL]_{eq}$	equilibrium concentration of complex
r	capillary radius
R	fraction of unbound ligand at equilibrium
t_1	the time span from the beginning of EM plug propagation to the time when the plug's center reaches the center of the detection window
t_2	time span from the plug center's passing the center of detection window to the end of plug propagation
t_3	time span from the beginning of electrophoresis to the moment when the center of the plug of PL reaches the center of the detection window
t_3'	varied value of t_3 by changing the electric field strength
t_{rebind}	characteristic rebinding time
t_{sep}	characteristic separation time of complex from unbound ligand and protein
v_{av}	pressure-driven velocity during the first passage
$\mathbf{v}_L$	electrophoretic velocity vector of ligand
v_L	electrophoretic velocity of ligand
$\mathbf{v}_P$	electrophoretic velocity vector of protein
$\mathbf{v}_{PL}$	electrophoretic velocity vector of complex
v_{PL}	electrophoretic velocity of complex during the second passage
φ	relative quantum yield of a fluorescent label within the protein–oligonucleotide complex with respect to that of the free oligonucleotide

Note S2: Calculating *R* from the velocity-corrected peak areas via double-passage approach

$$R = \frac{[\mathrm{L}]_{\mathrm{eq}}}{[\mathrm{L}]_0} = \frac{[\mathrm{L}]_{\mathrm{eq}}}{[\mathrm{PL}]_{\mathrm{eq}} + [\mathrm{L}]_{\mathrm{eq}}} = \frac{(\varphi[\mathrm{PL}]_{\mathrm{eq}} + [\mathrm{L}]_{\mathrm{eq}}) - \varphi[\mathrm{PL}]_{\mathrm{eq}}}{\{\varphi[\mathrm{PL}]_{\mathrm{eq}} / \varphi\} + \{(\varphi[\mathrm{PL}]_{\mathrm{eq}} + [\mathrm{L}]_{\mathrm{eq}}) - \varphi[\mathrm{PL}]_{\mathrm{eq}}\}} =$$

$$\frac{A_1 v_{\mathrm{av}} / a - A_2 v_{\mathrm{PL}} / a}{\{(A_2 v_{\mathrm{PL}} / a) / \varphi\} + \{A_1 v_{\mathrm{av}} / a - A_2 v_{\mathrm{PL}} / a\}} = \frac{A_1 v_{\mathrm{av}} - A_2 v_{\mathrm{PL}}}{A_2 v_{\mathrm{PL}} / \varphi + A_1 v_{\mathrm{av}} - A_2 v_{\mathrm{PL}}}$$

Note S3: Calculating k_{off} by varying *E* during the second passage

The value of k_{off} can be determined by using varying t_3 via changing the electric field strength ($E' < E$). A two-point approach (with two different values of t_3: $t_3 < t_3'$) can be used for a simple assessment of k_{off}:

$$1 - R(t_3) = (1 - R_{t=0}) e^{-k_{\mathrm{off}} t_3}, \qquad 1 - R(t_3') = (1 - R_{t=0}) e^{-k_{\mathrm{off}} t_3'}$$

$$\frac{1 - R(t_3')}{1 - R(t_3)} = e^{-k_{\mathrm{off}} (t_3' - t_3)}, \qquad \ln\left(\frac{1 - R(t_3')}{1 - R(t_3)}\right) = -k_{\mathrm{off}} (t_3' - t_3)$$

$$k_{\mathrm{off}} = \frac{\ln\left(\frac{1 - R(t_3)}{1 - R(t_3')}\right)}{t_3' - t_3}$$

Note S4: Recovery of peak areas

In order to evaluate the recovery of velocity-corrected peak areas via the double-passage approach, we used 1 µM GFP as an analyte mimicking PL in terms of electrophoretic mobility. The experiment was repeated 10 times using the default conditions: d = 10.2 cm, r = 37.5 µm, l = 1.09 cm, pressure equal to 0.30 psi, total capillary length = 50 cm, E = 200 V/cm (**Figure S1**). Detailed calculation for recovery of peaks areas can be found from **Table S1**.

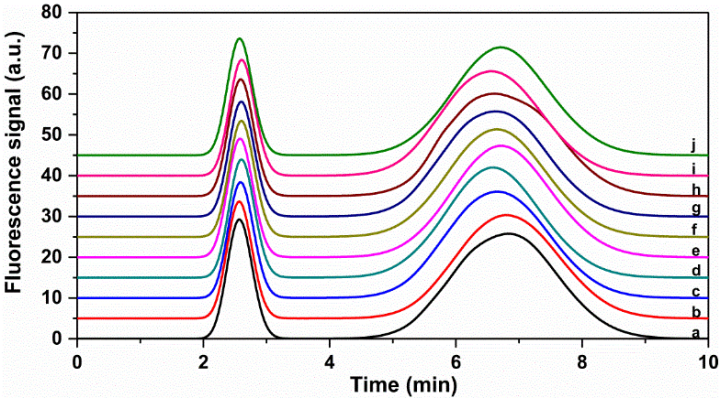

Figure S1. Double-passage experiment performed with 1 µM GFP in IFCE running buffer (50 mM Tris-HCl pH 7.0, 100 mM NaCl). Ten repetitions were done to determine the average velocity-corrected areas and to assess the error.

Table 1. Recovery of peak areas for double-passage experiment with 1 μM GFP

Figure	A_1	A_2	t_1 min	v_{av} cm/min	t_2 min	d_1 cm	t_3 min	v_{PL} cm/min	$(A_1v_{av})/(A_2v_{PL})$
S1, trace a	8.70×10^7	3.11×10^8	2.85	3.39	0.933	3.16	3.36	0.941	1.01
S1, trace b	8.43×10^7	2.91×10^8	2.85	3.39	0.933	3.16	3.28	0.963	1.02
S1, trace c	8.44×10^7	2.92×10^8	2.87	3.36	0.913	3.07	3.16	0.971	1.00
S1, trace d	8.60×10^7	2.92×10^8	2.88	3.35	0.900	3.01	3.11	0.969	1.02
S1, trace e	8.65×10^7	2.98×10^8	2.86	3.37	0.921	3.11	3.20	0.972	1.01
S1, trace f	8.41×10^7	2.92×10^8	2.88	3.35	0.900	3.01	3.14	0.959	1.01
S1, trace g	8.38×10^7	2.95×10^8	2.88	3.35	0.900	3.01	3.12	0.967	0.98
S1, trace h	8.48×10^7	2.89×10^8	2.88	3.36	0.908	3.05	3.11	0.981	1.00
S1, trace i	8.41×10^7	2.84×10^8	2.89	3.34	0.896	3.00	3.05	0.984	1.01
S1, trace j	8.40×10^7	2.92×10^8	2.85	3.38	0.929	3.14	3.21	0.980	0.99

See the accompanying Excel file for full data and error calculations

Note S5: Recovery of *R*

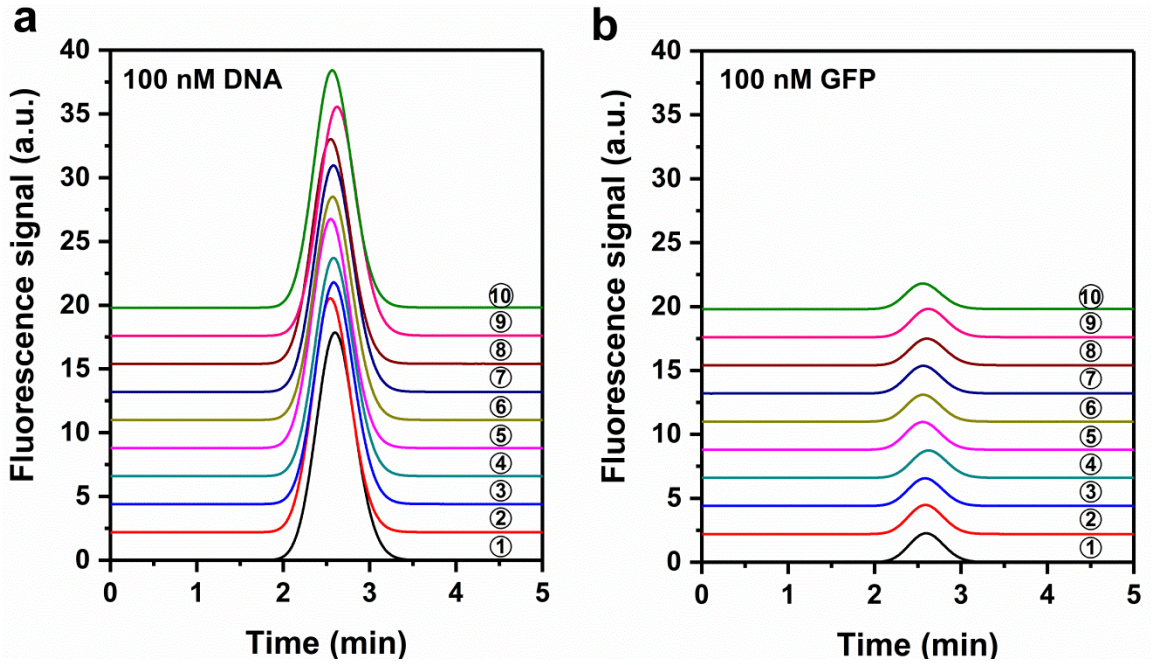

Figure S2. Determination of φ for GFP–DNA mixture. Areas of peaks of GFP and DNA yield a ratio of ≈0.11. Each set of experiments was performed 10 times. See the accompanying Excel file for full data and error calculations.

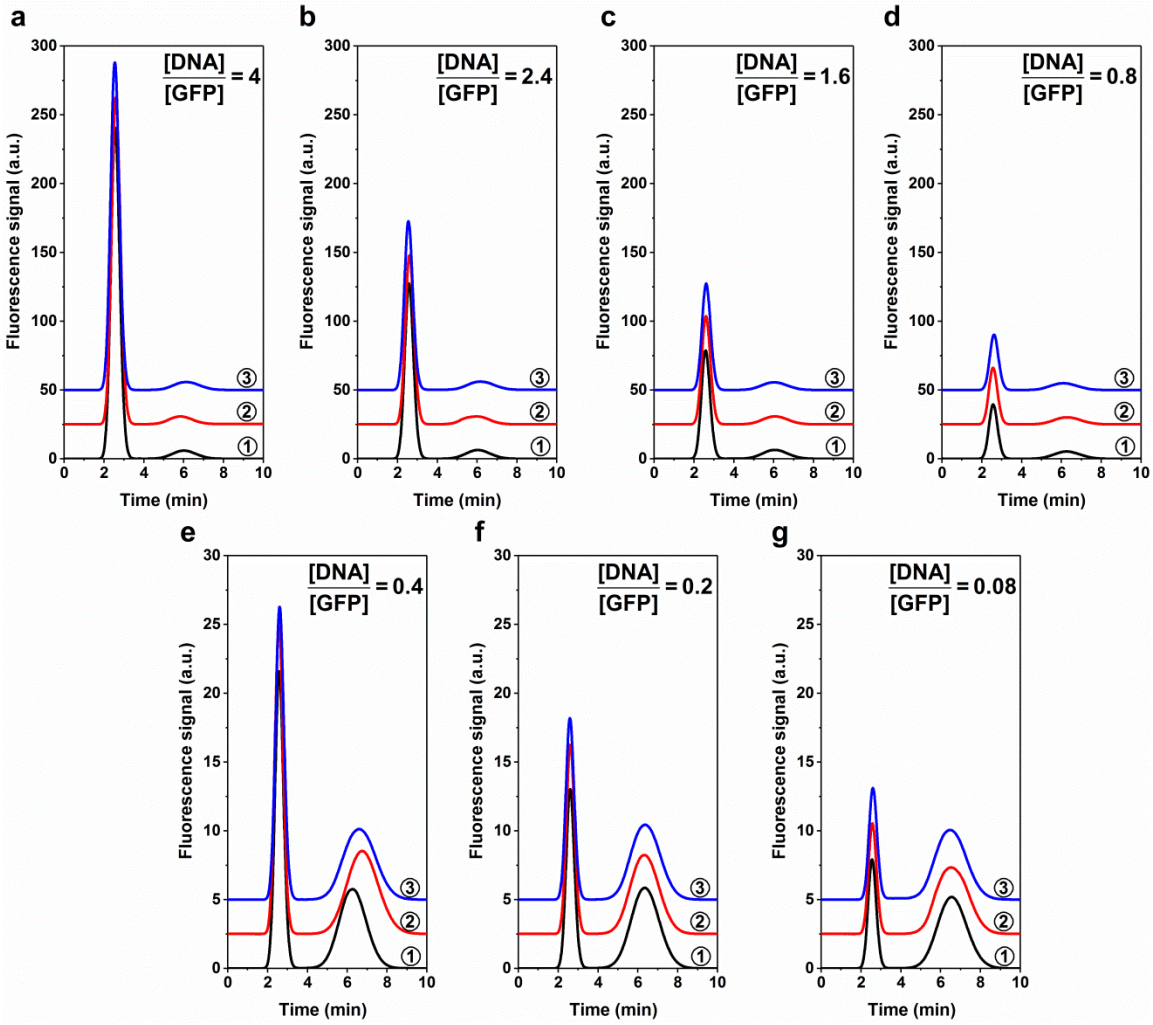

Figure S3. Double-passage experiments of GFP–DNA mixtures with [DNA]/[GFP] ratios ranging from 0.08 to 4. Each set of experiments was performed in triplicates.

Table S2. Recovery of *R* for double-passage experiment of GFP–DNA mixtures.

[DNA]/[GFP]	Figure	A_1	A_2	t_1 min	v_{av} cm/min	t_2 min	d_1 cm	t_3 min	v_{PL} cm/min	R	Mean R ± SD
	S3-a, 1	7.88×10^8	5.18×10^7	2.85	3.39	0.937	3.18	2.52	1.26	0.814	
4	**S3-a, 2**	7.84×10^8	4.93×10^7	2.88	3.36	0.908	3.05	2.34	1.30	0.815	0.813 ± 0.003
	S3-a, 3	7.79×10^8	5.44×10^7	2.83	3.41	0.954	3.26	2.64	1.23	0.810	
	S3-b, 1	4.15×10^8	5.70×10^7	2.86	3.37	0.921	3.11	2.54	1.22	0.677	
2.4	**S3-b, 2**	4.00×10^8	5.65×10^7	2.89	3.34	0.896	3.00	2.43	1.23	0.667	0.672 ± 0.005
	S3-b, 3	3.93×10^8	5.59×10^7	2.83	3.41	0.950	3.24	2.64	1.23	0.671	
	S3-c, 1	2.56×10^8	5.15×10^7	2.87	3.37	0.917	3.09	2.55	1.21	0.585	
1.6	**S3-c, 2**	2.56×10^8	5.40×10^7	2.88	3.35	0.900	3.01	2.58	1.17	0.580	0.582 ± 0.003
	S3-c, 3	2.51×10^8	5.23×10^7	2.90	3.34	0.888	2.96	2.52	1.18	0.581	
	S3-d, 1	1.27×10^8	5.13×10^7	2.85	3.39	0.933	3.16	2.76	1.15	0.411	
0.8	**S3-d, 2**	1.33×10^8	5.13×10^7	2.85	3.39	0.937	3.18	2.79	1.14	0.424	0.423 ± 0.011
	S3-d, 3	1.30×10^8	4.84×10^7	2.90	3.34	0.888	2.96	2.62	1.13	0.433	
	S3-e, 1	6.90×10^7	5.80×10^7	2.86	3.37	0.921	3.11	2.78	1.12	0.222	
0.4	**S3-e, 2**	7.00×10^7	7.03×10^7	2.85	3.38	0.929	3.14	3.23	0.97	0.213	0.225 ± 0.013
	S3-e, 3	6.71×10^7	5.97×10^7	2.89	3.34	0.896	3.00	3.08	0.97	0.240	
	S3-f, 1	4.06×10^7	6.12×10^7	2.88	3.35	0.900	3.01	2.85	1.06	0.108	
0.2	**S3-f, 2**	4.10×10^7	5.69×10^7	2.86	3.37	0.919	3.10	2.83	1.10	0.118	0.114 ± 0.005
	S3-f, 3	4.08×10^7	5.85×10^7	2.87	3.36	0.913	3.07	2.87	1.07	0.116	
	S3-g, 1	2.41×10^7	5.64×10^7	2.84	3.40	0.942	3.20	3.05	1.05	0.041	
0.08	**S3-g, 2**	2.43×10^7	5.73×10^7	2.86	3.38	0.925	3.12	3.03	1.03	0.041	0.042 ± 0.001
	S3-g, 3	2.48×10^7	5.85×10^7	2.88	3.35	0.900	3.01	2.99	1.01	0.043	

See the accompanying Excel file for full data and error calculations

Note S6: Experimental determination of K_d and k_{off} of protein–aptamer complex

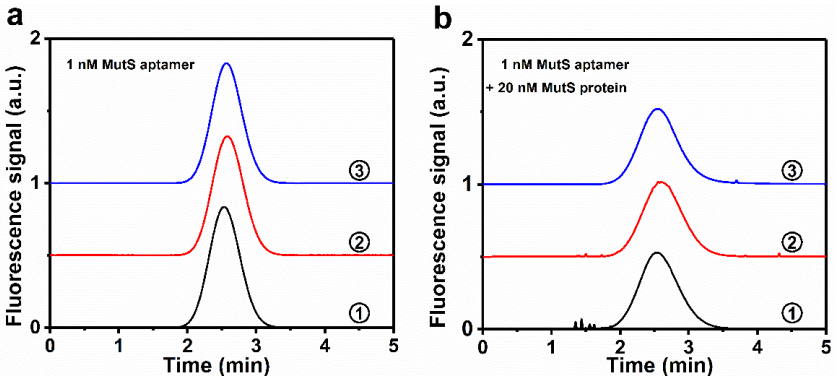

Figure S4. Determination of φ for MutS–aptamer mixture. Areas of peaks PL and L, at full complex saturation and at absence of target protein yield a ratio of ≈0.80. Each set of experiments was performed in triplicates. See the accompanying Excel file for full data and error calculations.

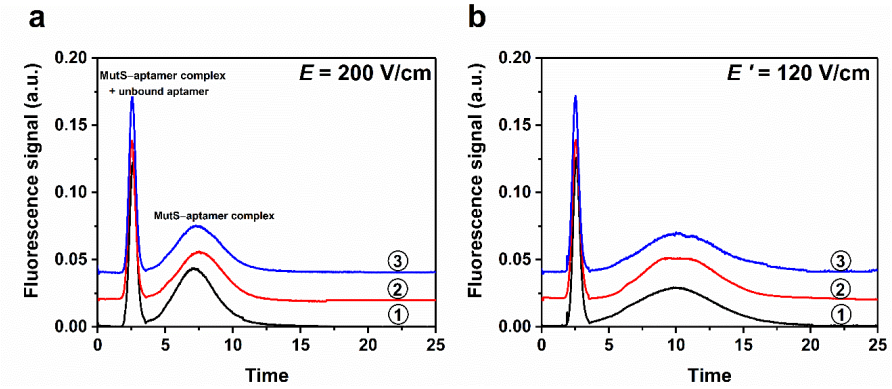

Figure S5. Double-passage experiment with mixture of MutS protein and its aptamer under different electric field strengths: (a) 200 V/cm and (b) 120 V/cm. Each set of experiments was performed in triplicates. The sample mixture contained 0.50 nM MutS and 0.20 nM aptamer**.**

Table S3. Experimental determination of K_d of MutS–aptamer complex

Figure	E V/cm	A_1	A_2	t_1 min	v_{av} cm/min	t_2 min	d_1 cm	t_3 min	v_{PL} cm/min	$R\varphi = 1$	$R\varphi = 0.80$	$K_d\varphi = 1$ nM	$K_d\varphi = 0.80$ nM
S5-a, 1		4.44×10^5	8.17×10^5	2.89	3.34	0.892	2.98	3.54	0.842	0.536	0.480	0.470	0.366
S5-a, 2	200	4.57×10^5	9.07×10^5	2.82	3.43	0.967	3.32	3.99	0.831	0.519	0.464	0.437	0.340
S5-a, 3		4.79×10^5	8.78×10^5	2.85	3.38	0.929	3.14	3.74	0.840	0.545	0.489	0.489	0.381
S5-b, 1		4.71×10^5	1.21×10^6	2.87	3.37	0.917	3.09	6.31	0.489	0.626	0.573	0.713	0.556
S5-b, 2	120	4.82×10^5	1.28×10^6	2.83	3.41	0.950	3.24	5.93	0.546	0.574	0.519	0.559	0.435
S5-b, 3		4.64×10^5	1.15×10^6	2.81	3.43	0.971	3.33	6.50	0.513	0.630	0.577	0.726	0.566

See the accompanying Excel file for full data and error calculations

Note 7: Determination of v_L

The value of v_L was determined by electrophoretically running a plug of pure L (MutS aptamer) with a cathode at the inlet using the following conditions: d = 4.4 cm, r = 37.5 µm, l = 1.09 cm, pressure equal to 0.30 psi, total capillary length = 50 cm, E = 200 V/cm (**Figure S6**). To achieve faster detection time of pure L under standard IFCE condition, the sample plug was propagated by injecting a 5.8 cm long plug of the run buffer with a pressure pulse of 0.3 psi × 90 s, resulting in a shorter d (4.4 cm). The value of t_4 was found directly from the electropherogram in **Figure S6**: t_4 = 714 s. The, the value of v_L = 0.006 cm/s was found with eq 21 in the main text.

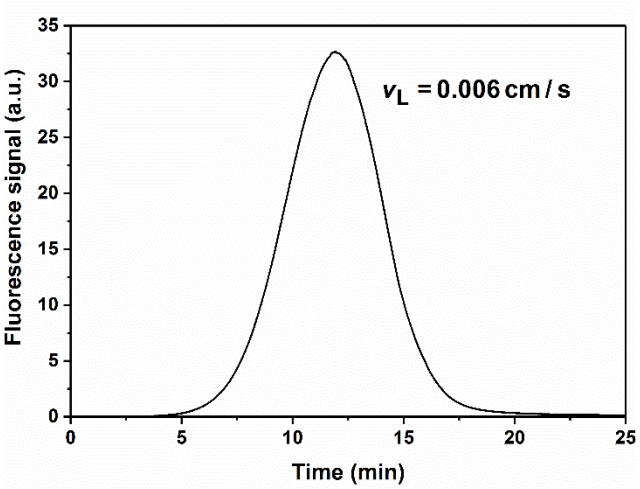

Figure S6. Determination of v_L. Concentration of L (MutS aptamer) was 50 nM.